International Journal of Science and Research (IJSR)
ISSN (Online): 2319-7064
Index Copernicus Value (2013): 6.14 | Impact Factor (2014): 5.611

FEA Optimization of Constructional Parameters of a Wind Turbine Blade Made of Composite Material

Tukesh Singh Thakur[1], Brijesh Patel[2]

[1]PG Scholar, Department of Mechanical Engineering, MATS University, Raipur, Chhattisgarh, India

[2]Mr. Assistant Professor, Department of Aeronautical Engineering, School of Engineering, IT, MATS University, Raipur, Chhattisgarh

Abstract: ***The overall goal of this project is to gain an understanding of wind turbine blades sufficient to develop Figures of Merit analysing the trade-offs between structure, material, cost, and other qualities in order to optimize the design of a large wind turbine blade. Due to the size of emergent utility-scale wind turbines, concerns that in current technology are minimal (such as weight), have the potential to add new dimensions to the driving design conditions. These additions are not necessarily captured by traditional wind turbine analytical solutions, and it has been wished to factor them into the analyses presented in the present work. In the due course of this project analytical solutions have been developed for various aerodynamic loads, along with rudimentary root size estimations. These analytic solutions have been used to guide the initial blade sizing and geometry, but transitioned to computational analysis tools like WT_Perf and ANSYS later on in order to more efficiently vary key design parameters and obtain additional accuracy in load profiles. Ultimately, optimization of several key design constraints for the blade has been done and computational results have been compared with initial analytic estimations to mixed results. Successful optimization of blade design has been done at key core levels. But detail many of the desired figures of merit have net been possible to develop. FOM has been obtained for structural stability and cost, but future work will be required to further evaluate these and others.***

Keywords: Wind Turbine, Aerofoil, Drag and Lift, Von-Misses stress, Optimization, ANSYS

1. Introduction

Today, as the world watches developing nations turn into industrial power-houses, many people are advising that these newly developed nations start with renewable energy resources in order to save money as well as prevent more greenhouse gasses from entering our world‟s atmosphere. Therefore, a renewable source, such as wind, is becoming a valuable resource around the world. India is just one example of a country that is exploring wind-generated power potential as a sustainable energy resource. In order to generate the large-scale wind farms, a few groups have come into the country to assess its potential as a wind-energy source and a few projects have been started. Domestic, foreign, and multi-international organizations have been selected as case studies for this report. Organizations like IWTMA (Indian Wind Turbine Manufacturers Association) have provided funding and research; Organizations like ReGenPowertech, Suzlon, RRB Energy Ltd, Inox Wind Ltd., Gamesa Renewable Pvt. Ltd., LM Wind power blade and many more are working tirelessly to produce and manufacture wind turbines in India. According to the Global Wind Energy Council website, wind power has grown steadily over the last decade, at an average rate of 30% annually. Worldwide, the use of wind turbines on agricultural land, on tops of mountain ridges, and in the oceans totals over 120 Gigawatt (GW) of energy generated. The largest in 2007 was the Enercon E126, which held a capacity of 6 megawatts (MW). The largest wind farm in the world is located in Texas and contains 420 turbines and produces 735 MW of energy. Together, the Asian market added nearly one third of the total new wind generators installed worldwide in 2008. In total, $50 billion was spent on turbine instillations worldwide that year. Almost half a million people are employed in some way by the wind energy industry and that number is growing steadily. With the current use of wind energy, over 158 million tons of carbon dioxide are saved from entering the atmosphere annually. Today, the United States leads with the world in wind energy generation, producing over 25,000 MW (Zervos, 2010). Wind energy is now being produced world-wide and developing nations have begun turning to wind powered renewable energy. India, however has a high potential for windpowered energy. As an emerging and developing country with a large land size, India is an excellent choice for renewable energy practices, according to The MNRE (Ministry of Non-conventional Energy Sources). Currently, coal is used as the major source of energy in the area because it is abundant and cheap. However, with the advancement of wind turbine technology and its widespread use and production, wind powered energy is becoming a cost effective way to harness energy sustainably. A sustainable energy resource is one that can be used renewably over our lifetimes and brings little to no impact on our world‟s ecosystems. The development of wind power in India began in the 1990s, and has significantly increased in the last few years. Although a relative newcomer to the wind industry compared with Denmark or the United States, India has the fifth largest installed wind power capacity in the world. In 2009-10 India's growth rate was highest among the other top four countries. The MNRE has announced a revised estimation of the potential wind resource in India from 49,130 MW assessed at 50m Hub heights to 102,788 MW assessed at 80m Hub height. The wind resource at higher Hub heights that are prevailing is possibly even more. In the year 2015, the MNRE set the target for Wind Power generation capacity by the year 2022 at 60,000 MW. As of 30 Sept 2015 the installed capacity of wind power in India was 24,376 MW, mainly spread across South, West and North regions. East and North east regions have no grid connected wind power plant as of March, 2015 end. No offshore wind power farm utilizing traditional fixed-bottom wind turbine technologies in shallow sea areas or floating

wind turbine technologies in deep sea areas is under implementation. The worldwide installed capacity of wind power reached 283 GW by the end of 2012. China (75,564 MW), US (60,007 MW), Germany (31,332 MW) and Spain (22,796 MW) are ahead of India in fifth position. The short gestation periods for installing wind turbines, and the increasing reliability and performance of wind energy machines has made wind power a favoured choice for capacity addition in India. Suzlon, an Indian-owned company, emerged on the global scene in the past decade, and by 2006 had captured almost 7.7 percent of market share in global wind turbine sales. Suzlon is currently the leading manufacturer of wind turbines for the Indian market, holding some 43 percent of market share in India. Suzlon's success has made India the developing country leader in advanced wind turbine technology.

The turbine blade design is guided perhaps most strongly by the flap wise bending moments. From (Manwell, McGowan, & Rogers, 2002), this moment is defined by

$$M_\beta = \frac{2}{3}\frac{T}{B}R$$

where T is thrust, B the number of blades, and R the radius of the turbine blade. The thrust coefficient (and from it, thrust) is a function of the axial induction factor a, and is defined by

$$C_T = 4a(1-a)$$

For the purposes of our analyses, we assumed the Betz limit of 1/3 for our axial induction factor. This represents a very conservative assumption, and accordingly drives up our expected moments beyond what would typically be expected for a blade of this size and type. Using these parameters and the relation between thrust and its coefficient, we determined the following for our blade:

Table 1: Aerodynamic Loads and Load Coefficients

	Rated Wind Speed (12 m/s)	Cut-out Speed (20 m/s)
a	.333	.333
CT	.889	.889
T	436 kN	1210 kN
Mβ	4.072 MN-m	11.31 MN-m
V	145 kN	404 kN

Additionally, we also sought to obtain the edgewise moment upon our blade. This moment is defined by the equation

$$M_E = \frac{Torque}{B} + W\frac{R}{3}$$

where M_E is the edgewise bending moment, and W the weight of the blade. Torque is simply the power of the turbine (1.5 MW) over the angular velocity (1.15 rad/s minimum, 1.76 rad/s maximum) of the blade. The moment arm here was assumed to be 1/3 the full blade length, in the belief that for a turbine blade with taper it is likely the center of mass lies between the blade root and midpoint. We also calculated the centrifugal force induced on the blade by its axial rotation. Where m is the mass of the blade, the relation is simply

$$F_c = mR\Omega$$

The mass of the blade in this first pass calculation was assumed to be 10 metric tons. The results from our findings can be seen in Table (2).

Table 2: Additional Aerodynamic Loads

	Low Rotational Velocity (1.15 rad/s)	High Rotational Velocity (20 m/s)
Torque	1.3 MN-m	.853 MN-m
ME	1.81 MN-m	1.66 MN-m
FC	484 kN	739 kN

Accordingly, we determined that the flapwise moment was indeed the key driver of our blade design, as the edgewise and centrifugal force terms are small in comparison. Using a blade design study from Sandia National Laboratory (TPI Composites, Inc., 2002), we were also able to determine the extreme loads for our blade when parked in 70 m/s winds. This calculation yielded a bending moment of 10.54 MN-m, a high value to be sure, but still lower than our very conservatively estimated flapwise bending moment.

An additional key design parameter that we determined was the necessary root thickness for our blade given the above load conditions. This thickness will be defined from our material properties, which can be seen below.

Table 3: Properties of Multidirectional QQ1 E-Glass Laminate (Samborsky, Wilson, &Mandell, 2007)

Property	Value (MPa)
Young's Modulus	33000
Tensile Strength	869
Compressive Strength	690

Generally speaking, the maximum stress of a body is related to the bending moment by the equation
where Iβ is the moment of inertia, and h the distance from the chordline, a quantity we will refer to as height. σmax is the material maximum stress, which for QQ1 E-glass in compression (and incorporating a safety factor of 2) is 345 MPa. For a hollow circular root section, the moment of inertia Iβ is defined as

$$I_\beta = \frac{1}{4}\pi(R_o^4 - R_i^4)$$

Accordingly, the thickness t of the blade can be calculated using the equation

$$t = R_o - \left(R_o^4 - \frac{4M_\beta h}{\pi\sigma_{max}}\right)^{1/4}$$

We were able to therefore calculate the necessary thickness for our blade root solely from the geometry and general performance characteristics of the blade. The resultant thicknesses from this analysis are given by Table (4).

Table 4: Necessary Blade Root Thickness at Rated and Cut-out Speeds

	Thickness (mm)
Rated Wind Speed (12 m/s)	3.78
Cut-out Speed (20 m/s)	10.6

These values represent our first pass at determining necessary blade geometry, and did not include such concerns as fatigue, additional materials, or internal components. Going forward, we will look at the effects such concerns have on these values.

Incorporation of Fatigue into Design Parameters

A given material's strength can decrease substantially over the course of its lifetime. Repeated loading and unloading of the material causes progressive and localized structural damage, and the resultant damage will lower the ultimate stress the material is able to endure without failure. This process of progressive material weakening is known as fatigue, and becomes an important design parameter when a material experiences many load cycles within its lifetime.

For a wind turbine, the expected life of a given blade may be estimated around 20 years. For this length of time, one can expect the blade to experience around 60 million load cycles. Examining the S-n curve for our blade material, it is possible to infer the ultimate limits of our blade for a 20 year lifetime. This fatigue limit can serve as an additional limiting factor for the analysis of our blade design.

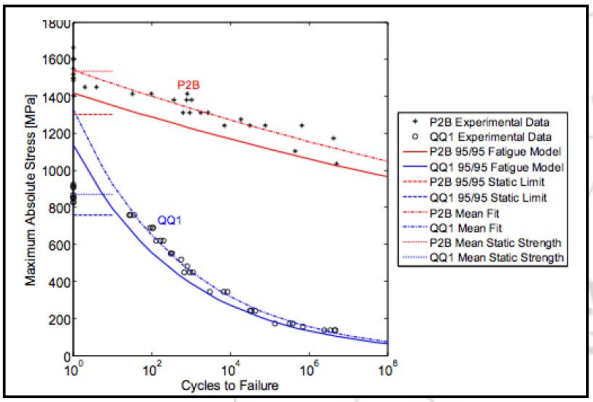

Figure 1: S-n Curve for QQ1 E-Glass and P2B Carbon/E-Glass Laminate (Samborsky, Wilson &Mandell, 2007)

2. Blade Material

As our blade is not a single material, we must look at how both the QQ1 E-glass and carbon laminate respond to fatigue limits. Using Figure (1), we are able to determine the following fatigued material limits for our blade.

Table 5: Fatigue Limits for Turbine Materials

	Maximum Allowable Stress at 60e6 cycles (MPa)
QQ1-E-glass	120
P2B Carbon Laminate	1200

As is expected, the ultimate stress of the fatigued carbon fiber is considerably higher than the allowable stress for the E-glass. Accordingly, the stress limit of the blade is determined by the strength of the E-glass used in the skin of the blade. As this fatigue limit occurs at the end of the expected lifespan of the turbine blade anyway, there is no need to incorporate an additional safety factor on this value, and we may assume the maximum allowable stress in our turbine blade to be 120 MPa.

It is worth noting that this stress value is below the one computed by our first pass analytic solution, so the necessary skin thickness of our blade is now higher than what was computed then. Updated thickness values for the first pass analytics are included in the table below.

Table 6: Necessary Blade Root Thickness at Rated and Cut-out Speeds (Incorporating Fatigue)

	Thickness (mm)
Rated Wind Speed (12	11.0
Cut-out Speed (20 m/s)	31.5

3. WT_Perf Methodology/Data

In order to determine the shape of the blade, we utilized a program developed by the National Wind Technology Center called WT_Perf. WT_Perf uses blade element momentum theory in order to approximate blade loading as well as the power output. The objective of the work with WT_Perf was to find a twist, chord, and airfoil configuration for a 41.25 m blade that produces 1.5MW in a wind speed of 10 m/s. The length, power output and wind speed come from the technical specifications of the GE 1.5 XLE wind turbine. The wind speed of 10 m/s is half the cut-out speed for the 1.5 XLE.

We used test file "Test04_WP15.wtp" as the starting point for our WT_Perf calculations. The test file uses 19 blade elements and three airfoils: S818, S825 and S826. It also uses the non-dimensional version of blade element momentum theory, which allowed us to easily scale our results to the specifications of the 1.5 XLE. Non-dimensional chord lengths and airfoil distributions were not changed, but we did have to iterate twist to achieve the desired power output. The optimal twist arrangement was found essentially by guess and check iteration. The table below displays the final geometry arrangement that was chosen.

Table 7: WT_Perf Blade Geometry

Element	r/R	Twist θ (in Degree)	C/R	Airfoil
1	0.075	42	0.0614	S818
2	0.125	32	0.06826	
3	0.175	23	0.07452	
4	0.225	15	0.07782	
5	0.275	11.5	0.07543	
6	0.325	8.2	0.07188	
7	0.375	7	0.06832	
8	0.425	6	0.06479	
9	0.475	5	0.06126	S825
10	0.525	4	0.05771	
11	0.575	4.15	0.05415	
12	0.625	3.85	0.05062	
13	0.675	3.25	0.04707	
14	0.725	2.75	0.0436	
15	0.775	1.25	0.04024	
16	0.825	0.75	0.03704	
17	0.875	0.55	0.03385	S826
18	0.925	0.85	0.03066	
19	0.975	0.05	0.02747	

The second column in the table above is the non-dimensional blade element position and the fourth column is the non-dimensional chord length. The table below displays the power output of a three blade wind turbine with the aforementioned geometry arrangement for rated wind speed (10 m/s) and cut-out wind speed (20 m/s) for various pitch angles.

Table 8: WT_Perf Power Output for Given Blade Geometry

Pitch (deg)	Power [kW] with 10 m/s wind	Power [kW] with 20 m/s wind
-4	1502.381	1541.013
-3	1550.928	2010.38
-2	1596.825	2488.243
-1	1623.915	2961.509
0	1627.014	3413.535
1	1611.397	3834.488
2	1580.034	4227.44
3	1535.555	4581.086
4	1480.177	4863.556

Additionally, we sought to determine the flapwise moment given by Wt_Perf, as this should be a more accurate calculation than that given by equation (1) from (Manwell, McGowan, & Rogers, 2002). The flapwise moments for our turbine are given below for rated, cut-out, and extreme wind speeds.

Table 9: Flapwise Moments from WT_Perf

	Rated Wind Speed 10 m/s	Cut-out Wind Speed 20 m/s	Extreme Winds 70 m/s wind
Pitch (deg)	0	0	82
M_β (kN-m)	2212	2875	96.7

The flapwise moments generated can thus be seen to be smaller than those calculated by equation (1). This is to be expected, however, as those moment values were calculated assuming an axial induction factor of 1/3. This represents the most conservative estimate possible to generate a given amount of power, and drives up the thrust quantity (and from that, M_β) considerably. Notably, the moment generated by extreme winds can be driven down significantly by pitching the blades appropriately into the wind. Were the blade to have no pitch (0 degrees), the moment in extreme winds would be 7386 kN-m. So long as we are able to pitch our blade, however, it is possible to keep even extreme winds from damaging the turbine blade.

4. Transformation of WT_Perf Loads

The loads given by WT_Perf are incredibly useful in providing a comprehensive numerical analysis of the edge and flapwise forces at a variety of operating conditions, allowing for an analysis of blade element loads given different blade pitch, wind speed, and more. These loads are all given in the local coordinates of the airfoil, however, and are thus not useful in applying appropriate load conditions within ANSYS, which operates by default in a global coordinate system.

The loads given by WT_Perf must therefore be transformed into their equivalent forces in the global coordinate system. In order to understand this transformation, it is probably best to define the system as follows:

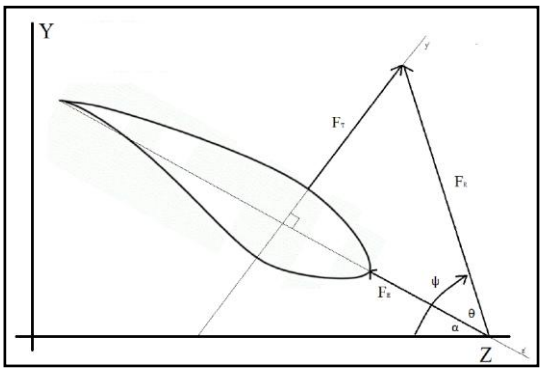

Figure 2: Airfoil Aero Forces and Relevant Transformation Geometries (not to scale)

As seen above, the thrust and edge forces are orthogonal, meaning the resultant force in the local coordinate system can be computed using Pythagoras' Theorem, or

$$F_R = \sqrt{F_T{}^2 + F_E^2}$$

This resultant force is oriented at some angle within the local coordinate system, and is defined by the length of its component sides, FT and FE. This angle is given by θ is the resultant force angle in the local coordinate system, but the local coordinates are themselves offset by some angle α, or the twist for that airfoil section. This twist angle is known from our WT_Perf data, as it is the twist angle given for that airfoil element. The angle Ψ as seen in Figure (2) is the angle that defines the orientation of FR in the global coordinate system, and is simply θ plus α. The resultant force acting in the global coordinate system has components FY and FZ, which are defined by the equations

$$F_Z = F_R \cos(\psi)$$
$$F_Y = F_R \sin(\psi)$$

5. Modelling of Turbine Blade

The analysis of the blade in an analytical fashion yields useful first-pass results about stresses and moments, which is useful in determining basic strength and material requirements. This type of analytical analysis, though useful, is insufficient to properly evaluate the full wind turbine blade.

Accordingly, we sought to use finite element analysis to more accurately capture the loads and stresses generated on the blade geometry by particular loading scenarios. This computational method allows for much greater flexibility in testing out various loads and blade geometries, allowing for an iterative approach to developing our turbine blade.

First, we began by selecting our airfoils. We decided to use the NREL S-series of airfoil as described in (Malcolm and Hansen 2006). These airfoils are in general somewhat thicker than the types typically seen on airplanes due to structural concerns, and are largely insensitive to roughness. As such, they are well suited for turbine blades.

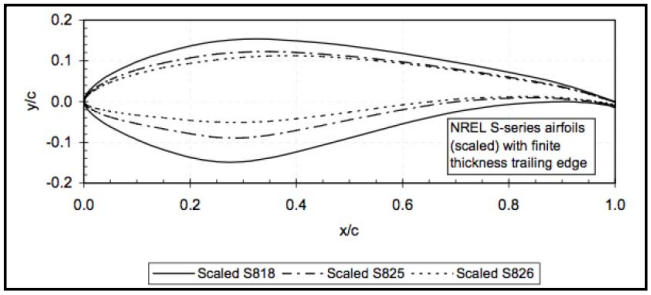

Figure 3: Turbine Blade Airfoils (S818, S825, S826)

The beginning of the blade is the circular hub section. This circular root transitions into the S818 airfoil, which then transitions to the S825 airfoil, which then transitions into the S826 airfoil used at the tip. The full blade geometry, including twist, span, and chord lengths, were determined through WT_Perf analysis and can be seen below.

Table 10: Turbine Blade Geometry

Relm (% span)	Span (m)	Twist (deg)	Chord (% span)	Chord (m)	Airfoil
0.075	3.09375	42	0.06140	2.5328	
0.125	5.15625	32	0.06826	2.8157	
0.175	7.21875	23	0.07452	3.0740	
0.225	9.28125	15	0.07782	3.2101	
0.275	11.34375	11.5	0.07543	3.1115	
0.325	13.40625	8.2	0.07188	2.9651	S818
0.375	15.46875	7	0.06832	2.8182	
0.425	17.53125	6	0.06479	2.6726	
0.475	19.59375	5	0.06126	2.5270	
0.525	21.65625	4	0.05771	2.3805	
0.575	23.71875	4.15	0.05415	2.2337	
0.625	25.78125	3.85	0.05062	2.0881	
0.675	27.84375	3.25	0.04707	1.9416	
0.725	29.90625	2.75	0.04360	1.7985	S825
0.775	31.96875	1.25	0.04024	1.6599	
0.825	34.03125	0.75	0.03704	1.5279	
0.875	36.09375	0.55	0.03385	1.3963	
0.925	38.15625	0.85	0.03066	1.2647	
0.975	40.21875	0.05	0.02747	1.1331	S826
1	41.25	0	0.02424	1	

With the full blade geometry defined, we began the process of building the blade for our FEA model. While it is possible to model and analyze a full wing using just ANSYS, we decided to model the blade using the SolidWorks CAD package instead due to familiarity with that program. As it is possible to import geometry directly from SolidWorks into ANSYS, this seemed to be the most efficient way to manage the creation of the blade.

In order to ensure maximum flexibility and computational efficiency within ANSYS, we designed the blade within SolidWorks as a lofted surface, which is analogous to building with ANSYS' shell elements. Blade design is essentially accomplished by pasting each airfoil element on a plane placed the appropriate distance from the turbine hub (the span distance seen in Table (10). Then, using the surface loft command, it is possible to connect these various sketches into a single body, letting SolidWorks automatically generate the intermediate blade shape between each defined airfoil. To minimize unnecessary complications in the geometry, we lofted each section using the airfoil leading edge as the loft guide point.

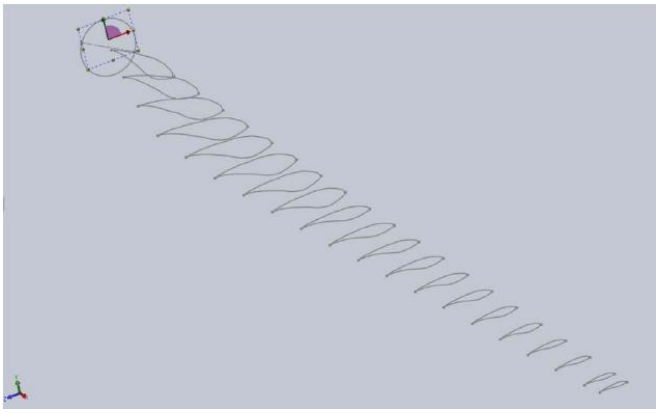

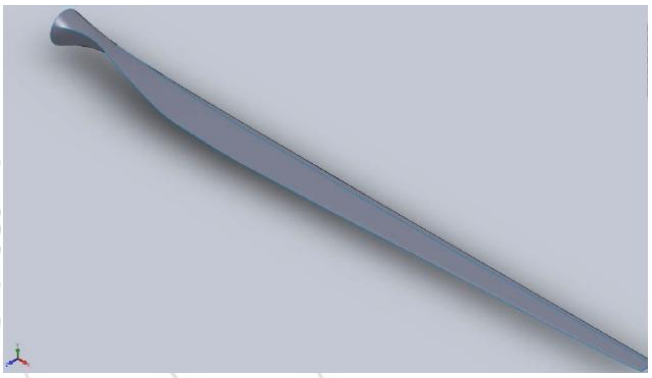

Figure 4: Full Blade Skeleton and Blade as a Lofted Surface

6. FEA Simulation and Optimization

This section will serve to describe how the full blade simulation was created in ANSYS. Many difficulties were encountered during the process, so the solutions will be outlined here.

Geometry The geometry for the wind turbine blade was created within SolidWorks. As we wished to work with ANSYS shell elements for computational efficiency, the SolidWorks model (consisting of 3 parts – top half of airfoil, bottom half of airfoil, and spar) was created using surface lofts. The completed SolidWorks blade was then imported into the ANSYS Design Modeler as a "frozen". It was important to import the geometry as a "frozen", as this allowed the geometry to be partitioned.

We partitioned the model so that we could apply different loads at different sections of the blade. It was decided to partition the blade into 5 equal spanwise segments. The length of the full blade is 41.25 m, so the length of each of the five segments was 8.25m. In order to partition the blade, a special extrusion feature was used. For instance, imagine that the span of the blade falls on the x axis, with the root at the origin. In order to make the first division, a rectangle was drawn on the YZ plane that could encompass the cross section of the blade. Next, the rectangle was extruded to 8.25 m, except the "operation" of the extrusion was set to "slice material". In order to make the next division, a plane parallel to the YZ plane was created at x=8.25m. Then a rectangle was drawn on this plane and extruded with the "slice material" operation. This, procedure was then repeated two more times in order to create the five partitions. Figure (5) shows the geometry of the model after partitioning.

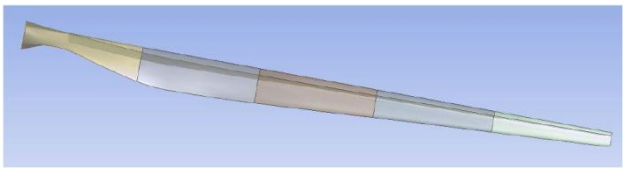

Figure 5: Full Blade Partitioned into Sections

After the geometry was partitioned the parts had to then be put together. For each spanwise partition there are three pieces: a top airfoil half, bottom airfoil half and spar. Thus, there were 15 pieces in total. In order to form one cohesive part out of the 15 pieces, you highlight all of the pieces in the tree outline, right click, and select "Form New Part". The formation of the single part is a very important step; if it is not taken the simulation will not work.

Prior to discussing the meshing, it must be mentioned that ANSYS creates false "Connections" when importing the geometry into the Mechanical editor. There should be no "Connections" as all the 15 pieces should be the constituents of one cohesive part. Thus, the faulty "Connections" were simply deleted. In order to delete the faulty "Connections", the "Connections" label in the tree outline was expanded and all of the "Connections" within were deleted. Next, mesh sizing commands were given to each of the five partitions. For each partition a "Body Sizing" command was implemented. The three parts of each partition (bottom half, top half and spar) were applied as the geometry of the "Body Sizing" command. Once, the five "Body Sizing" commands were implemented the resolution of the mesh could be manipulated with ease. The following picture shows a course mesh in which the element size for all five "Body Sizing" commands was set to 0.6m.

Figure 6: Full Blade with Coarse Mesh

The advantage of having "Body Sizing" commands for each section is that one section can be given higher resolution. For instance, in Figure (7) the element size for the root section was set to 0.3m, whereas the element size for the four other "Body Sizing" commands were set to 0.4m.

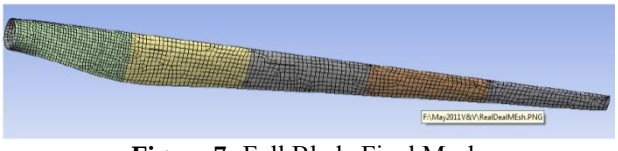

Figure 7: Full Blade Final Mesh

It can be seen that there are significantly more elements in the root section than the other four sections, which is useful due to the complicated geometry of the root transition from circular hub to S818 airfoil. This was the mesh used for the final simulations.

ANSYS does not have a feature in its GUI that allows varying of shell thickness as a function of position. In order to incorporate varying thicknesses we used command "Snippets". For each of the fifteen pieces of the wing geometry a command "Snippet" was needed. These command "Snippets" specified the material properties as well as thickness for that particular piece. ANSYS defines equations in three dimensional matrices. Thus, in order to specify a thickness one must first create the three dimensional matrix that defines the desired thickness equation. In order to create the equation matrix, the older form of ANSYS, Mechanical APDL, was used. The equation matrices were found by defining functions within the "Function Tool" in APDL and saving the file. The saved files were then opened with a text editor where the three dimensional matrices can be found. The matrices were then copied into the command "Snippets" in order to define the thickness function. It must also be mentioned that one additional command "Snippet" was placed in the analysis portion of the simulation. This last command "Snippet" essentially forbids ANSYS from overriding anything that was specified in the previous command "Snippets".

For the simulation, the root section of the blade was fixed using the "Fixed Support" command. In order to apply the loads to the blade a "Force" command was created for each of the five partitions. The "Force" commands were applied to the top and bottom half of the blade for each section. The forces on each blade section were then defined in component form (the FZ and FY values obtained using WT_Perf).

We wished to iterate our blade design to obtain a blade that incorporated as little material as possible while still meeting key design criteria. The basic premise was to apply the loading for the cut-out speed of 20 m/s to the blade and adjust the thickness of each of the three parts such that these design constraints were satisfied.

The first design limit ensures that the blade could not hit the turbine tower. It was estimated that the blade was 4 m away from the tower at the hub. Turbine blades, however, are generally inclined such that the blade is angled away from the tower when pointing towards the ground. Using a blade inclination of 5 degrees, we determined that the deflection of the blade tip could not exceed 7.6 meters.

The second design constraint was that the stress in the spar could not exceed 1200 MPa, the fatigue limit of P2B carbon laminate. The final design limit was that the stress cannot exceed 120 MPa, the fatigue limit of QQ1 E-glass, in the skin of the blade. The design of the blade and its iterations focused primarily on the deflection and skin stress design limits, as the stress within the carbon fiber spar never approached its limit. The root section of the blade was fixed and the five sections were given the following loading, which is based on the WT_Perf data for the 20 m/s wind speed case.

Table 11: Full Blade Section Forces – Cut-out Wind Speed

Section	FY (N)	FZ (N)
1	5868	345
2	14763	447
3	23445	2828
4	33908	7184
5	39321	8791

The spar was given a Young's Modulus of 101 GPa and the blade halves were given a Young's Modulus of 33 GPa. First we varied the spar thickness to determine what was needed to

limit the total deformation to fall below 7.6m. Next, the skin thickness functions were varied to ensure the stress remained below 120MPa. The optimal configuration turned out to be a constant spar thickness of 10 cm and a linearly varying thickness for the blade. The optimal thickness equation for the blades was a linear function with 30 mm thickness at the root and 10 mm thickness at the tip. The aforementioned thicknesses and loading yielded the following deformation and normal stress respectively.

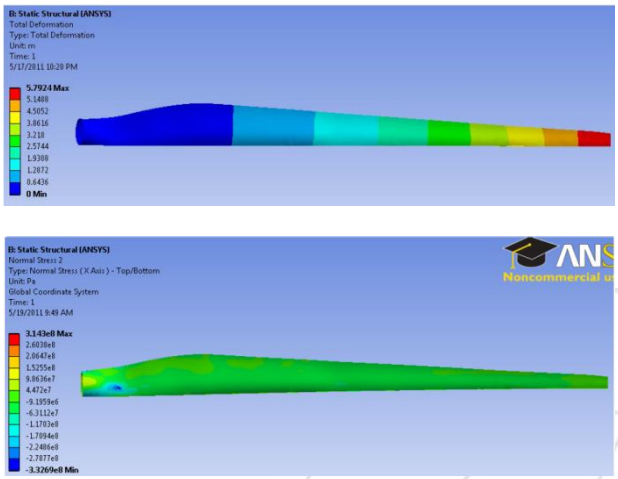

Figure 8: Full Blade Deformation and Stress for Cut-Out Wind Speed

It can be seen that ANSYS calculates a stress concentration approximately 3m from the blade root. This concentration is due to the contact between the beginning of the spar and blade and can be neglected. Aside from this small stress concentration where the spar begins, the stresses within the blade fall well below the design criterion. The deformation also falls well below the design limit with a value of 5.79m.

After optimized thicknesses were found we re-ran the simulations run for the rated case of 10 m/s wind. The loading for this case (based on WT_Perf) is shown by Table (12).

Table 12: Full Blade Section Loads – Rated Wind Speed

Section	FY (N)	FZ (N)
1	4923	436
2	13723	1715
3	22725	1981
4	30324	2516
5	24521	1766

These loading conditions yielded the following results in ANSYS for deformation and normal stress respectively.

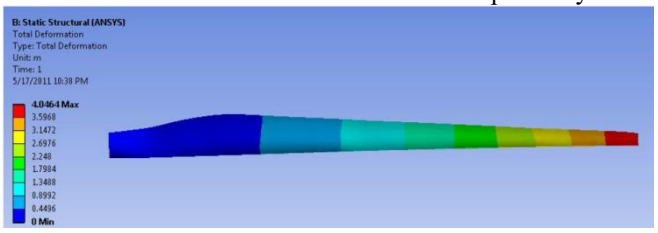

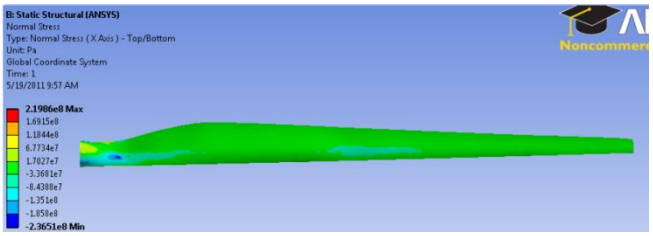

Figure 9: Full Blade Deformation and Normal Stress for Rated Wind Speed

Once again the small stress concentration appears at the start of the spar, and once again we neglect this inflated stress value. Throughout the remainder of the blade the stress is far below the maximum skin stress, and the deformation within its limits. Thus, the optimal spar thickness for our blade is a constant 10 cm and the optimal skin thickness is a linearly varying function with a root thickness of 30mm and a tip thickness of 10mm.

7. Result And Discussion

After deciding upon the blade geometry and material properties, it was of interest to compute a first pass estimate of the material cost for the blade. In order to calculate this value, we first determined the total mass of used of each blade component. The mass of spar was found to be 3030 kg and the total mass of the skins was found to be 9940 kg. Assuming that the carbon laminate can be purchased for $11/kg and that QQ1 E-glass can be purchased for $2/kg, the cost of the blade materials would be $53,210.

We were able to effectively model our blade and optimize it to minimize material use while maximizing material and design specifications. Also of interest, however, was how this computational result compared with those values obtained from our analytical solutions.

As shown in Table (6), when we use the flapwise bending moment obtained from the equation (1) analytic solution for Mβ, the blade thickness should be 31.5mm. The moment used here, however, is an estimation based on the maximum value for the axial induction factor. Accordingly, this solution results in what should be an overbuilt blade root. Using the flapwise bending moment obtained from WT_Perf (Mβ =2.875 MN-m) and equation (7), we find that the necessary thickness should be 7.71mm.

However, it is important to note that, again, WT_Perf load are all done in local coordinates. The flapwise moment calculated is thus not necessarily what was input into ANSYS. The flapwise moment using the ANSYS global coordinate system can be determined through statics, using the FY values from Table (10) and the average span distance from the section in question. The total flapwise moment is merely a summation of these induced section moments, and equals 3.361 MN-m. Using the thickness equation, the necessary root thickness would then be 9.04mm. A comparison of the various moments can be seen below:

Table 13: Necessary Root Thicknesses for Various Conditions (at cut-out wind speed, fatigue incorporated)

	M_β (MN-m)	Thickness (mm)
Moment derived analytically from Betz limit	11.31	31.5
Moment given in WT_Perf	2.875	7.71
Moment from ANSYS loads	3.361	9.04
ANSYS Model	3.361	30.0
Extreme winds (70 m/s) with 0° pitch	7.386	20.2

Table (13) shows the flapwise bending moments and the necessary thicknesses they incur from the analytic solution for thickness (the exception being the ANSYS model thickness, which was optimized within the program for that root thickness). It is interesting to note that the calculated thickness closest to what is actually required comes from the analytic solution where the moment was derived from the Betz limit axial induction factor. All other analytic solutions underestimate the necessary skin thickness at the root. Though the Betz limit derived moment yields a value close to what we actually determined from our computations, the similarity seems serendipitous given the significant difference in the flapwise moment. Given the data, it seems likely that our first pass analytic solution for thickness generally underestimates the necessary thickness needed at the root. The extreme winds case, for instance, still yields a necessary thickness less than the Betz limit derived moment case or ANSYS given thickness.

After the optimal blade configuration we were able to calculate the mass of the blade. The blade is made out of QQ1-E-glass and P2B carbon laminate with densities of 2.53g/cm3 and 1.78 g/cm3, respectively. We defined these densities within ANSYS, and applied them to the appropriate sections of the blade. We then defined a skin thickness of 20mm and a spar thickness of 100mm. This approximation of skin thickness (which varies along length) had to be done, as ANSYS will not read thickness values from command "Snippets" for mass calculation. 20mm was chosen as it is the average thickness of the skin (which varies from 30mm to 10mm along the span of the blade). With material densities and thicknesses applied, ANSYS reported a total blade mass of 12,969 kg. This yields a weight of 127.2 kN, and the maximum edgewise moment is therefore 2.07 MN-m. The edgewise moment input into the ANSYS model can be calculated similarly to the flapwise moment, performing a summation of FE multiplied by moment arm for each section. The comparison of edgewise moments can be seen in Table (14).

Table 14: Edgewise Bending Moment Comparison

	ME (MN-m)
Analytic Solution	2.07
ANSYS Model	.637

In the analytic solution, it is worth noting that now the edgewise bending moment has increased from our first-pass solution due to the increased weight of the blade. The moment calculated is still small compared to the Betz limit derived flapwise moment, but is relatively high compared to the WT_Perf and ANSYS model flapwise moments. Even assuming those smaller values for Mβ, however, the flapwise moments remain the main drivers for structure. The ANSYS model edgewise moment is notably small, which is likely due to the absence of weight as a factor. In the analytic solution for instance, the weight driven moment term actually accounted for around 86% of the moment. So while the weight from a large turbine may not be a driving design factor from a structural standpoint, it is nonetheless the driving factor in the value of the edgewise moment.

References

[1] ANSYS. (n.d.). Mechanical APDL Verification Manual.
[2] Beer, F. P., Johnston, E. R., &DeWolf, J. T. (2006). Mechanics of Materials (4th Edition ed.). New York, NY: McGraw-Hill.
[3] Grande, J. A. (n.d.). Wind Power Blades Energize Composites Manufacturing. Retrieved December 12, 2010, from PlasticsTechnology: http://www.ptonline.com/articles/200810fa2.html
[4] Lawrence, K. L. (2010). ANSYS Workbench Tutorial. SchroffDevelopement Corporation.
[5] Manwell, J. F., McGowan, J. G., & Rogers, A. L. (2002). Wind Energy Explained: Theory, Design and Application. Chichester, NY: Wiley.
[6] Materials Database. (n.d.). Retrieved December 1, 2010, from Matbase: http://www.matbase.com/material/fibres/glass/e-glass-fibre/properties
[7] Nolet, S. C. (2010, March 10). Manufacturing of Utility-Scale Wind Turbine Blades. Retrieved December 12, 2010, from Iowa Wind: http://www.iawind.org/presentations/nolet.pdf
[8] Samborsky, D. D., Wilson, T. J., &Mandell, J. F. (2007). Comparison of Tensile Fatigue Resistance and Constant. AIAA .
[9] Stress in Thick-Walled Tubes or Cylinders. (n.d.). Retrieved October 19, 2010, from The Engineering ToolBox: http://www.engineeringtoolbox.com/stress-thick-walled-tube-d_949.html
[10] The Windpower. (2010). Retrieved November 16, 2010, from http://www.thewindpower.net/fiche-eolienne-technique-58-ge-energy-1.5xle.php
[11] TPI Composites, Inc. (2002). Parametric Study for Large Wind Turbine Blades. Warren, RI: Sandia National Laboratory.
[12] Composite / Steel Cost Comparison. MIT Materials Systems Laboratory. Retrieved 05/19/2011 http://msl1.mit.edu/MIB/3.57/LectNotes/gm_tech_composites.pdf
[13] http://wind.nrel.gov/airfoils/
[14] http://www.indianwindpower.com/publications.html#tab5
[15] Peter J. Schubel and Richard J. Crossley Wind Turbine Blade Design. Energies 2012, 5, 3425-3449; doi:10.3390/en5093425
[16] http://www.mdpi.com/search?q=&journal=energies&volume=&authors=&section=&issue=&article_type=&special_issue=320&page=&search=Search